RESEARCH ARTICLE

Macromolecular Rapid Communications

www.mrc-journal.de

3D Printable Conducting and Biocompatible PEDOT-*graft*-PLA Copolymers by Direct Ink Writing

*Antonio Dominguez-Alfaro, Elena Gabirondo, Nuria Alegret, Claudia María De León-Almazán, Robert Hernandez, Ainara Vallejo-Illarramendi, Maurizio Prato, and David Mecerreyes**

Tailor-made polymers are needed to fully exploit the possibilities of additive manufacturing, constructing complex, and functional devices in areas such as bioelectronics. In this paper, the synthesis of a conducting and biocompatible graft copolymer which can be 3D printed using direct melting extrusion methods is shown. For this purpose, graft copolymers composed by conducting polymer poly(3,4-ethylenedioxythiophene) (PEDOT) and a biocompatible polymer polylactide (PLA) are designed. The PEDOT-*g*-PLA copolymers are synthesized by chemical oxidative polymerization between 3,4-ethylenedioxythiophene and PLA macromonomers. PEDOT-*g*-PLA copolymers with different compositions are obtained and fully characterized. The rheological characterization indicates that copolymers containing below 20 wt% of PEDOT show the right complex viscosity values suitable for direct ink writing (DIW). The 3D printing tests using the DIW methodology allows printing different parts with different shapes with high resolution (200 µm). The conductive and biocompatible printed patterns of PEDOT-*g*-PLA show excellent cell growth and maturation of neonatal cardiac myocytes cocultured with fibroblasts.

1. Introduction

Additive manufacturing (AM) has drawn tremendous attention as a versatile platform for the on-demand fabrication of objects with excellent special control and functionality. The development of polymeric materials that are tailor made for AM is highly desirable for a variety of applications ranging from tissue engineering, biomedical devices, aerospace, energy, or soft robotics.[1,2] As recently highlighted by Nelson and Narupai, "the future of additive manufacturing will depend on new polymeric materials that are specifically designed for these technologies."[3] As a representative example, ionic and/or electronic conducting polymers which are 3D printable are actively being searched nowadays for next-generation (bio)electronic devices. Poly(3,4-ethylenedioxy thiophene), known as PEDOT, has become the most popular electronic conducting polymer for many reasons, including its commercial availability, transparency as thin films, conductivity, and stability. In particular, in the field of bioelectronics, PEDOT is used in many different devices ranging from scaffolds,[4] biosensors,[5] ion pumps,[6] cutaneous electrodes,[7] or organic electrochemical transistors.[8] However, PEDOT as a conjugated polymer is insoluble and infusible, which limits its processability. In most cases, PEDOT dispersions using stabilizers such as polystyrene sulfonate is formulated in the form of inks and processed using conventional solvent casting approaches such as spin-coating, inkjet, or screen printing. Compared to other polymers, PEDOT limited processability resulted in unsuccessful early processing attempts via additive manufacturing methods. Only recently, Zhao and

Dr. A. Dominguez-Alfaro, E. Gabirondo, Dr. N. Alegret, Dr. C. M. De León-Almazán, Dr. R. Hernandez, Prof. D. Mecerreyes
POLYMAT University of the Basque Country UPV/EHU
Avenida de Tolosa 72, Donostia-San Sebastián 20018, Spain
E-mail: david.mecerreyes@ehu.es

Dr. A. Dominguez-Alfaro, Prof. M. Prato
Carbon Bionanotechnology Group
Center for Cooperative Research in Biomaterials (CIC biomaGUNE)
Basque Research and Technology Alliance (BRTA)
San Sebastian 20014, Spain

Dr. N. Alegret, Dr. A. Vallejo-Illarramendi
IIS Biodonostia, Neurosciences Area
Group of Neuromuscular Diseases
Paseo Dr. Begiristain s/n, San Sebastián 20014, Spain

Dr. A. Vallejo-Illarramendi
Group of Neuroscience
Department of Pediatrics
Faculty of Medicine and Nursing
UPV/EHU, Paseo Dr. Begiristain 105, San Sebastian 20014, Spain

Prof. M. Prato
Department of Chemical and Pharmaceutical Sciences
INSTM – University of Trieste
Via L. Giorgieri 1, Trieste 34127, Italy

Prof. M. Prato, Prof. D. Mecerreyes
Ikerbasque
Basque Foundation for Science
Bilbao 48013, Spain

The ORCID identification number(s) for the author(s) of this article can be found under https://doi.org/10.1002/marc.202100100

DOI: 10.1002/marc.202100100

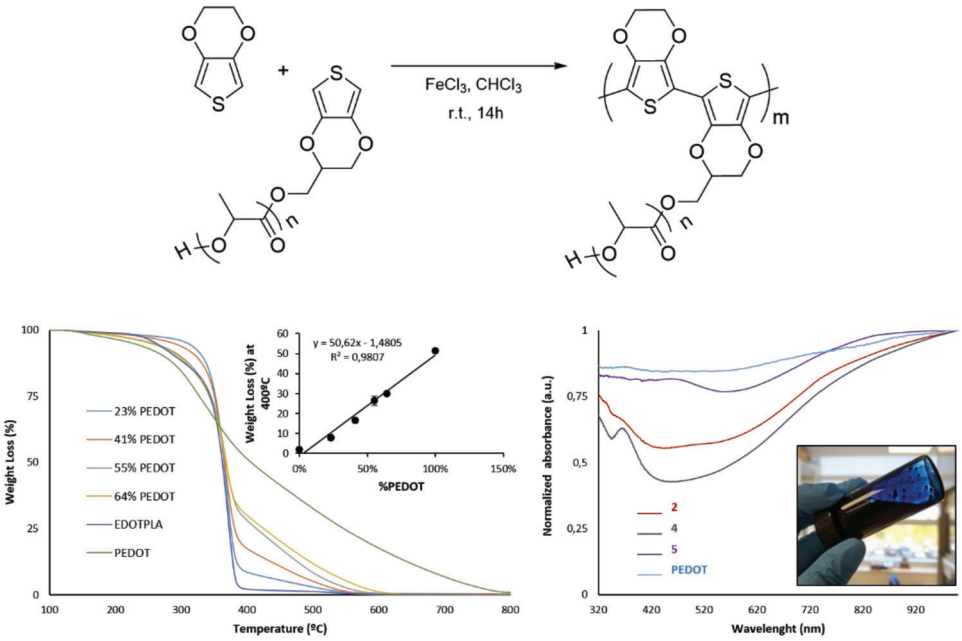

Figure 1. (Top) Reaction scheme of synthesis of PEDOT-*g*-PLA by chemical oxidative copolymerization; (Bottom) TGA of the blends formed for the calibration line and UV–vis of different PEDOT-*g*-PLA copolymers.

co-workers have designed PEDOT/polystyrene sulfonate (PSS) inks with characteristic shear thinning and shear yielding properties for AM. Through direct 3D printing of these inks, hydrogel and dry conductive microscale structures were demonstrated.[9] On the other hand, using light as a processing method, 3D printable conductive hydrogels were developed by Zhang and co-workers based on PEDOT/PSS and a polyethylene glycol (PEG)-diacrylate that could be photocrosslinked while retaining high electrical conductivity. The conductive hydrogel was patterned on the substrate by using a table top stereolithography (SLA) 3D printer.[10] Besides these examples, examples of other popular AM technologies based on polymer melting methods such as filament fused fabrication (FFF) or direct ink writing (DIW) were not known.[11] In this line, Müller and co-workers recently reported the use of classical polymer processing techniques, including melt extrusion followed by fiber spinning or fused filament 3D printing for PEDOT/Nafion composite.[12]

Polylactide (PLA) is the most popular biobased and biocompatible polymer, which is commonly 3D printed by FFF methods for biomedical applications.[13] For this reason, we selected PLA to be combined with PEDOT to develop conducting materials that could be 3D printed using melting processing. Although the easiest and most straightforward method would be to prepare blends of both homopolymers, we decided to copolymerize them to combine their properties intimately and avoid miscibility issues. For this reason, in this paper we targeted the synthesis and characterization of graft copolymers of PEDOT-*g*-PLA as 3D printable materials endowed with electronic conductivity and biocompatibility.

2. Results and Discussion

The PEDOT-*g*-PLA copolymers were synthesized, as shown in **Figure 1**, by chemical oxidative copolymerization between 3,4-ETHYLENEDIOXYTHIOPHENE (EDOT) and PLA macromonomer. The macromonomer method was previously reported as a successful methodology for the synthesis of conductive graft copolymers between different thermoplastic polymers such as polyesters or poly(meth)acrylates and conducting polymers such as PEDOT or polypyrrole.[14–18] For this purpose, we first synthesized three different PLA macromonomers of molecular weights between 7000 and 24 000 g mol^{-1} by organocatalyzed ring-opening polymerization of L,L-lactide initiated by EDOT-methanol (Table S1, Supporting Information). The characterization of the macromonomers by ^{1}H nuclear magnetic resonance (NMR) spectroscopy and matrix-assisted laser desorption ionization-time of flight (MALDI-TOF) spectroscopy (Figure S1, Supporting Information) confirmed the presence of the EDOT end group. Besides, the performance of the catalysts in bulk polymerization was evaluated by ^{13}C NMR, resulting in atactic PLA due to the known racemization process during the bulk polymerization reaction. Then, the oxidative copolymerization between EDOT and EDOT-PLA macromonomer was carried in chloroform using $FeCl_3$ as oxidant. A blue dispersion was obtained after the polymerization, which shows the typical UV bipolaron[19] absorption in the near-IR of conducting PEDOT as shown in Figure 1. The PEDOT-*g*-PLA copolymers were then purified and recovered as powders by precipitation. **Table 1** summarizes the copolymerization results and the characteristics of PEDOT-*g*-PLA copolymers. As observed, the final composition of the copolymers is related to the feed composition between EDOT and PLA in the reaction mixture and a set of copolymers with varying ratio between PEDOT and PLA were obtained. The PEDOT composition in the graft copolymer could be qualitatively estimated by Fourier transform infrared (FTIR) spectroscopy, by comparing the different bands associated to the homopolymers that appeared in the copolymer spectra (Figure S2, Supporting

Table 1. Copolymerization of EDOT with PLA macromonomers in $CHCl_3$ at room temperature for overnight.

Entry	PLA[a] macromonomer	W_{PEDOT}[b] [wt%]	W_{PEDOT}[c] (IR)*	Yield [wt%]	σ[d] [μS cm^{-1}]
1	1a	5	14	50	5.1 ± 0.2
2	1b	5	11	60	1.8 ± 1.0
3	1b	10	20	45	8.9 ± 0.1
4	1b	15	27	38	20.1 ± 1.5
5	1b	40	74	25	208.4 ± 17
6	1c	5	13	53	2.9 ± 0.2
7	1c	10	19	40	22.6 ± 4.1
8	1c	40	71	20	300 ± 24.1

[a] PLA macromonomers M_n calculated by ^{1}H NMR; [b] Weight fraction of EDOT in the reaction feed; [c] Weight fraction of PEDOT in the copolymers as calculated by TGA; [d] Electrical conductivity of PEDOT-*g*-PLA measured by four-point probe.

Information). Then, PEDOT and PLA weight composition was calculated by thermogravimetric analyses (TGA) (Figure S3, Supporting Information). The composition of PEDOT-*g*-PLA copolymers could be estimated by developing a calibrating line with weight loss versus PEDOT percentage. The PEDOT composition in the final graft copolymer was higher than the one in the reaction feed, similarly than previously observed for other similar graft copolymers such as PPy-*g*-PCL.[16] As expected, PEDOT-*g*-PLA copolymers present electrical conductivity as shown in Table 1. Higher electrical conductivity was obtained as the PEDOT content in the copolymers increased. In all the cases, the conductivity values were in the order of (μS cm^{-1}) similar than previous examples of conducting polyester graft copolymers.[15,20] It is worth to note that although the values are relatively low as compared to pure conducting PEDOT:PSS those are higher than conducting coatings of PEDOT:PSS on PLA/PHBV fibers (from 0.22×10^{-8} and 1.45×10^{-8} S cm^{-1}).[21] Moreover, our PEDOT-*g*-PLA copolymer is in the same order of magnitude of typical conducting PLA composites with carbon nanotubes PLA/MWCNT (3.5×10^{-5} S cm^{-1}).[22] It is worth to note that the conductivity values shown in Table 1 may be good enough for tissue engineering applications. As previously reported, da Silva et al. PEDOT-*co*-PDLLA with similar conductivity values, induce the differentiation of stem cells into neurons, showing an improvement with respect to the neurofilament lengths of those neurons increased up 370% compared to control. Besides, the correlation between the nanoscale electrical surface of the copolymer and the production of fibronectin, protein key role in the fibrillogenesis among other regulatory processes, was also confirmed for this range of conductivity.[15]

The PEDOT-*g*-PLA copolymers were further characterized by transmission electron microscopy (TEM) to evaluate their particle morphology. As shown in Figure S4 (Supporting Information), PEDOT obtained under similar synthetic conditions is a powdery material with particle sizes close to 1 μm. By increasing the amount of PLA in the copolymers, the PEDOT-*g*-PLA powders show small particle size, as shown by TEM (<100 nm). Films were prepared by solvent casting and observed by scanning electron microscopy (SEM). Interestingly, whereas the PEDOT and the 40:60 wt% PEDOT-*g*-PLA copolymer film show an inhomogeneous aspect, the copolymer 5:95 wt% PEDOT-*g*-PLA (2) shows a homogeneous surface by SEM. This copolymer possesses an aspect similar to a PLA macromonomer film obtained by this method, which anticipates that it may show similar printing properties. SEM and TEM observations are in line with PEDOT copolymerization with cationically charged PEDOT-N recently reported where PEDOT confers higher particles size and partially loss of the solubility.[23]

The initial PLA macromonomers and the PEDOT-*g*-PLA copolymers were further characterized by differential scanning calorimetry (DSC). Figure S5 (Supporting Information) shows the DSC scans for PLA7K macromonomer and its PEDOT copolymer (1). Within the first heating scan, two peaks can be observed in both materials: glass transition temperature (T_g) and melting temperature (T_m) at 53 and 110 °C, respectively. It is worth to note that the melting temperature and crystallinity of the PLA is lower than typically observed for a poly(L-lactic acid) (PLLA) material. This is due to the synthetic route of the macromonomer which uses high temperatures which induce the racemization during the polymerization leading to PLA ≈70% atactic. The polymers were cooled down at very low rate (1 °C min^{-1}) (Figure S5b, Supporting Information). In the second heating scan only T_g is observed associated with the PLA phase without a sign of melting or crystallization. Moreover, copolymers with higher PEDOT composition such as (i.e., 5 and 8) resulted did not show any T_m. The phase separation between the PEDOT and PLA in the graph copolymers was also investigated by atomic force microscopy (AFM). The AFM images (Figure S6, Supporting Information) show phase separation between a continuous phase which can be assigned to the amorphous PLA region which is the main constituent of the graft copolymer and spherical domains of nanometer size of PEDOT (Figure S15, Supporting Information). Unfortunately, the AFM analysis could not be carried out to all the copolymer compositions, since at higher PEDOT content the samples showed low solubility and high surface roughness. All in all, the phase separation occurs in the nanometer scale which ensures the intimate mixing between the two polymers as it was previously observed in the case of similar conducting graft copolymers.

Rheological measurements were carried out at 110 °C above the melting temperature of the graft copolymers. PLA homopolymer and PEDOT copolymers presented rheological complex behavior. Generally, copolymers with low PEDOT percentages or high molecular weight present the loss modulus (G'') that exceeds the storage modulus (G') at low frequencies indicating the viscous nature, while for copolymers with higher amount of PEDOT and low molecular weight, G' exceeds G'' indicating its dominant elastic nature. Accordingly, complex viscosity (η^*) of the starting macromonomers and the PEDOT-*g*-PLA at different compositions have been represented comparatively in **Figure 2** to evaluate the impact of PEDOT in the copolymers and its further printability. Thus, complex viscosity for PEDOT percentages higher than 25% presents values higher than 10 000 Pa s that correspond to viscoplastic behavior, where storage modulus (G') higher than loss modulus (G'') (Figure S7, Supporting Information). This solid-like behavior is responsible of poor flow and eventually blocking printed nozzle. However, macrostructures with lower molecular weight and copolymers with PEDOT composition between 15 and 20, present η^* between 1000 and

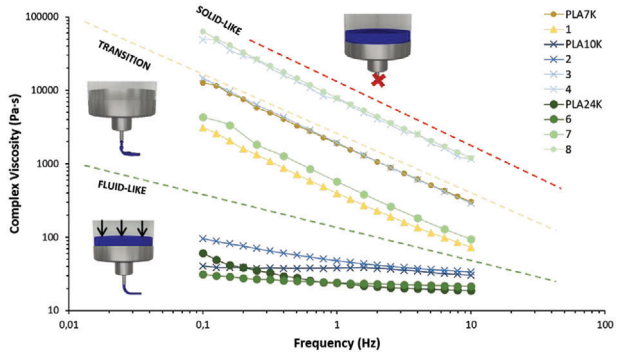

Figure 2. Complex viscosity at 110 °C of initial PLA macromonomers and resulting PEDOT-*g*-PLA graft copolymers (entry 1–8 of Table 1) measured in frequency studies.

10 000 Pa s, hence a transition between solid and liquid. This behavior presents some difficulties to flow and require the addition of a physical input to be used in printed inks. Finally, materials with low viscosities present slightly shear thinning behavior, that is, homopolymers and graft copolymers with PEDOT content below 13%, that possess η^* ranged between 100 and 1000 and represent the most suitable compositions for flowing and further printability test. This observation was also confirmed by the comparative observation between loss and storage modulus presented in frequency sweeps in Figure S7 (Supporting Information).[24]

DIW 3D printing tests were carried out using an extrusion printer, where the PEDOT-*g*-PLA powder was placed inside a metallic extruder, warmed up to melting temperature, and extruded by the action of compressed air. Then, the material in its fluid-like state was deposited in a desired shape that instantaneously solidified on the bed at room temperature, in the same way than PLA homopolymers. Besides, 3D-printed homopolymer and PEDOT copolymer were characterized rheologically, and they did not present degradation or evidences of partial hydrolization of the PLA by the dual action of air and temperature (Figure S8, Supporting Information). Indeed, isothermal analysis at melting temperature in air atmosphere indicates better thermal stability of graft copolymers than homopolymer, due to the presence of PEDOT in the polymer chains (Figure S9, Supporting Information). **Figure 3** shows the graphical representation of the printed process as well as some pictures of the different structures printed. In the upper left part, a SEM picture of an interdigitated layer-by-layer printed image is shown while in the bottom part different examples of PEDOT-*g*-PLA designs with different shapes are presented standing out the good resolution of the printing process. Moreover, samples of the different copolymers after printing were evaluated by DSC (Figure S10, Supporting Information). After printing the copolymers were fully amorphous without any crystallization and showing one glass transition at around 55 °C associated with the PLA phase.

Figure 4 shows the SEM images of the interlayer area of the printed compositions. PEDOT-*g*-PLA (copolymer 1) required the action of physical input (piston) and higher pressures due to its plastic behavior. It also required larger nozzle of around 0.5 mm inner diameter, decreasing the printing quality. In contrast, PEDOT-*g*-PLA (copolymer 6) presented a lower complex viscosity, hence, lower pressures were needed. Nevertheless, the deposited layer tends to expand and partially lose its shape. It is remarkable that copolymer with 20 wt% of PEDOT composition (7) and higher molecular weight was printed using the physical action of the piston, this composition presented better printing performance than his predecessor 6 and it was able to keep the shape. Figure S11 (Supporting Information) shows the interlayer topography of copolymer 3 that present a roughly topography mostly composed of particles. Finally, 5:95 wt% PEDOT-*g*-PLA (copolymer 2) presented the best performance during the printing process, improving the ability to control its shape. Also, the easy flow allowed the use of a smaller nozzle (0.2 mm inner diameter) in the printing process. Although slightly layer contraction was still observed, PEDOT-*g*-PLA copolymer 2 (Table 1) presented an excellent flow resistance. Therefore, it was chosen as the patterning material for biocompatibility tests on neonatal cardiac cultures.

Interestingly, previous works have demonstrated that PEDOT-PLA possess dual biocompatibility and electronic conducting which is very useful in cell culture of bidimensional films with stem cells or electrospun fibers with skin fibroblasts.[21] In our case, the selected PEDOT-*g*-PLA copolymer 2 was patterned in hexagonal and striped shapes for cardiomyocytes and fibroblast coculture. Cardiomyocytes present a more mature phenotype when cultured on specific shapes.[25,26] Hence, the performance of nonconducting PLA patterns was compared to PEDOT-*g*-PLA patterns to evaluate the effect of the PEDOT and electronic conductivity of the material. The cell growth and maturation was analyzed within material and between the interstices of hexagonal (1–5 mm diagonal) and stripped pattern structure (200–400 µm space). Some small differences in the surface morphology between printed PLA and PEDOT-*g*-PLA patterns can be observed in Figure S12 (Supporting Information).

Primary ventricular cardiomyocytes (CM) and cardiac fibroblasts (CF) isolated from the hearts of neonatal mice were cultured during 7 d and high biocompatibility was observed. The most significant difference between the PLA and PEDOT-*g*-PLA patterns reside in the ability of NMVM to produce extracellular matrix (ECM) between the interstices and printed conductive pattern. Remarkably, such observed pre-tissue is actively beating (see Video S1, Supporting Information).

The morphology of the cultured cells was analyzed by staining the sarcomere of the CM with alpha-actinin and the CF microtubules with antivimentin. **Figure 5** corroborates the attachment of CM and CF to the materials and fibrous ECM generated in the PEDOT-containing structures. In addition, the cells incubated on the PEDOT-*g*-PLA patterns present a mature phenotype, i.e., a rectangular shape and an organized sarcomeric pattern (Figure 5 and Figure S12, Supporting Information). Furthermore, fibrous large elongations of fibroblasts along the fibrous ECM formed and abundant cell-to-cell contacts are also clearly distinguished in PEDOT-*g*-PLA interstices. This suggests that the cardiomyocytes are able to maintain their typical morphology and their structural supporting function when growing on PEDOT-*g*-PLA patterns. It further supports the potential of our material to facilitate the generation of artificial tissue. On the other hand, the cardiac cells grown within PLA-patterned interstices are comprised of nonelongated fibroblasts and star-like cardiomyocytes, which is the typical shape of immature neonatal

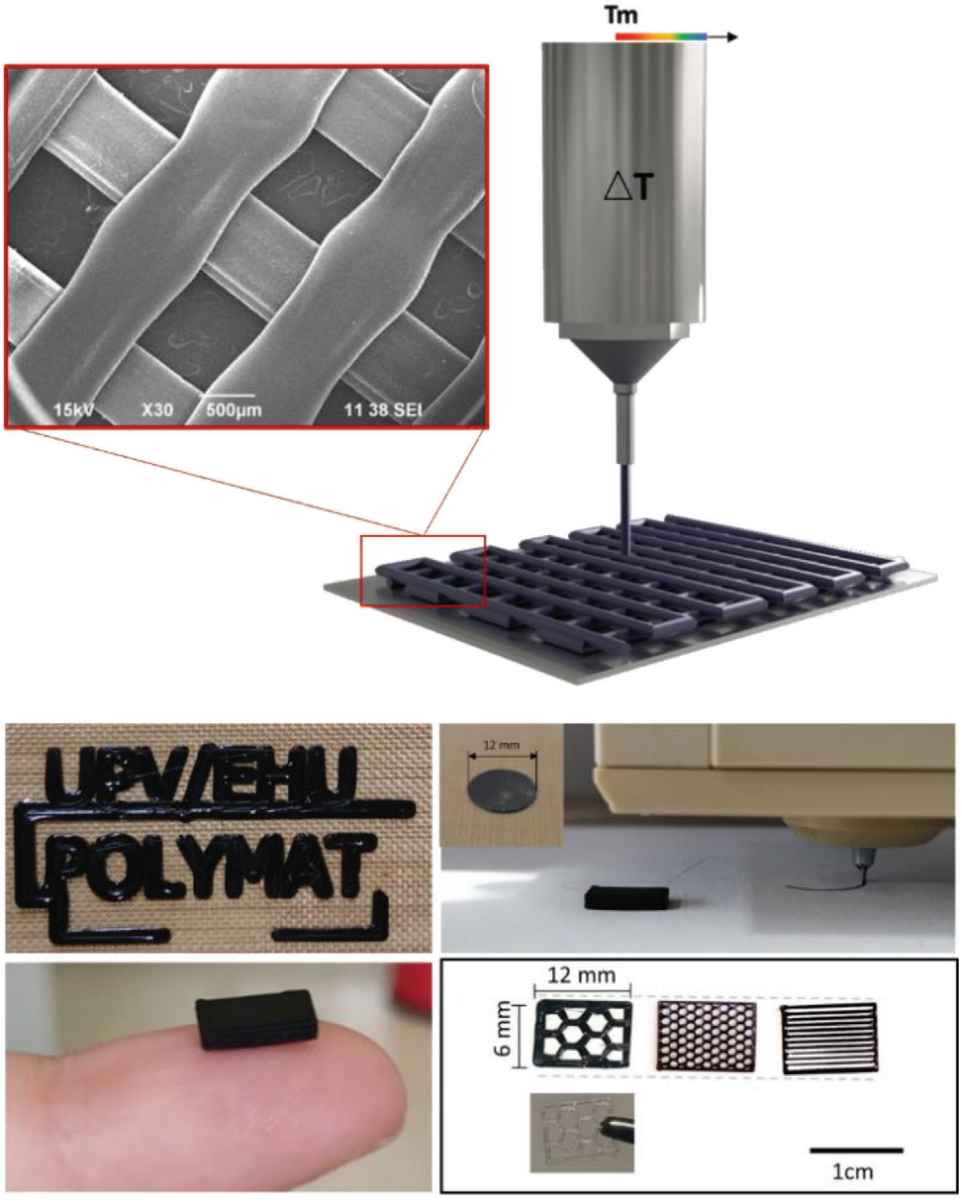

Figure 3. Upper left image: SEM image of a printed micropattern. Bottom images: Different geometries printed by melting extrusion including patterns used for biocompatibility tests.

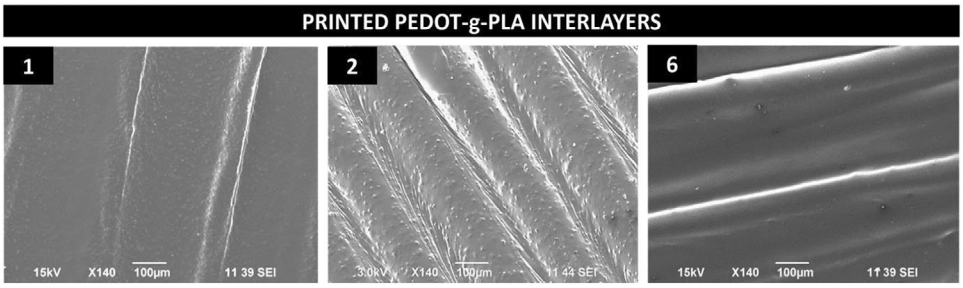

Figure 4. SEM images of the 3D-printed PEDOT-*g*-PLA copolymers with 5% EDOT in the feed.

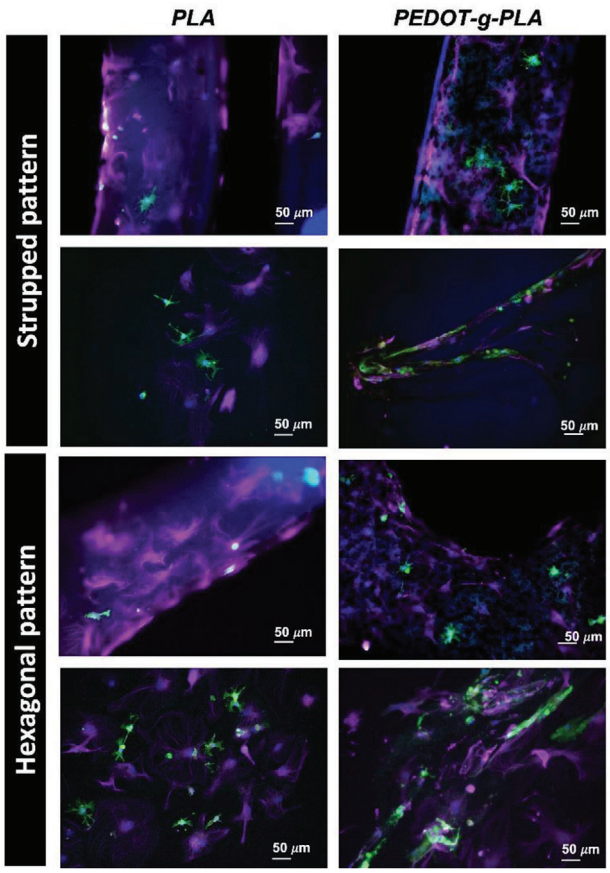

Figure 5. Immunofluorescence images of CM and CFs cocultures grown on printed PLA and PEDOT-*g*-PLA stripped and hexagonal patterns for 7 d. Antibody staining against α-actinin (green) and vimentin (pink) label CM and CF, respectively, with nuclei labeled using DAPI (blue).

cardiac cells grown in culture (see controls in Figures S13 and S14, Supporting Information). Regarding the printed material, the growth of fibroblasts is abundant and extend in both PLA and PEDOT-*g*-PLA surfaces. However, cardiomyocytes are more abundant on the PEDOT-containing substrate, suggesting a better attachment of the CM and a higher biocompatibility of the conductive substrate (Figure S15, Supporting Information). Remarkably, tissue-like structures composed of cardiomyocytes and CFs were generated in the PEDOT-*g*-PLA patterns while random growth was observed in control PLA patterns. Overall, all these observations suggest the presence of viable and functional cardiomyocytes which are not observed in the absence of PEDOT.

3. Conclusions

In conclusion, we have described a new conducting PEDOT copolymer that can be printed by direct ink writing though melting extrusion. A series of graft copolymers between PEDOT and biocompatible PLA were investigated. Complex viscosity by frequency oscillatory studies at the melting temperature suggest two different behaviors, solid-like behavior for higher PEDOT percentages ($G' > G''$) and liquid-like for lower ($G'' < G'$) for compositions lower than 10 wt%. In accordance, the copolymers with low PEDOT content were able to flow and printed by melt extrusion. The PEDOT-*g*-PLA with a PEDOT composition between 11 and 14 wt% were patterned in hexagonal and striped shapes to culture cardiomyocytes and cardiac fibroblast. Good biocompatibility was observed and tissue-like structures composed of cardiomyocytes with fibroblast were developed in PEDOT-*g*-PLA while random growth was observed as control in PLA. Moreover, cardiomyocyte beating confirmed proper maturation and functionality of these cells. All in all, this work shows the successful design of a conducting and biocompatible PEDOT-*g*-PLA material for melting extrusion 3D printing.

4. Experimental Section

Materials: L,L-lactide (99%) was supplied by Purac, and it was recrystallized before using it. 1,8-Diazabicyclo[5.4.0]undec-7-ene (DBU) was purchased from TCI, and it was distilled before its use. EDOT and benzoic acid (BA) were provided by Sigma-Aldrich and were used without further purification.

Synthesis of the PLA Macromonomer: The reactions were prepared mixing previously synthesized DBU:BA organocatalyst (5 mol%), lactide and hydroxy methyl EDOT initiator in a vial with a magnetic stirrer. The sealed reaction vessels were submerged into a preheated oil bath at 130 °C until 90% of monomer conversion was obtained, 1.5 h. The reactions were stopped by rapid cooling in liquid nitrogen. The purification of the macromonomer was done by dissolving them in chloroform and precipitating in methanol. Finally, they were dried under vacuum at RT for 24 h.

Synthesis of DBU:BA Organocatalyst: DBU:BA catalyst was prepared using the following procedure. First, BA was placed in a flask with ether. Once the acid was completely dissolved DBU base was added dropwise to the solution obtaining a white salt. The salt was filtered and washed with excess of ether and dried under vacuum.

Synthesis of PEDOT-g-PLA copolymers: Graft copolymers of various compositions were prepared via chemical oxidative copolymerization of EDOT and PLA macromonomers using $FeCl_3$ as oxidizing agent and $CHCl_3$ as a solvent. In a typical composition of 95PLA:5EDOT (wt%), PLA_{10k} (1.5 g, 1.47×10^{-4} mol) and EDOT (0.078 g, 5.492×10^{-4} mol) were dissolved in 10 mL of $CHCl_3$. After mixture was totally dissolved, 0.135 g of $FeCl_3$ (1.5 eq EDOT monomer) was added. Immediately, the reaction turned dark and after few minutes into dark blue. The reaction was left overnight and collected by precipitation. The blue solution was precipitated and washed in methanol until the iron residue was fully removed. The product was finally dried under vacuum at room temperature.

Methods: Nuclear Magnetic Resonance Spectroscopy: *^{1}H and ^{13}C NMR Spectroscopies*: ^{1}H NMR spectra were used for analyzing the macromonomer conversions and the copolymer final composition. ^{13}C NMR spectra were used to determine the tacticity. ^{1}H and ^{13}C NMR spectra were recorded with a Bruker Advance DPX 300 at 300.16 and 75.5 MHz resonance frequency, respectively, using $CDCl_3$ as solvents at room temperature. Experimental conditions were as follows: a) ^{1}H NMR spectroscopy: 10 mg of sample; 3 s acquisition time; 1 s delay time; 8.5 μs pulse; spectral width 5000 Hz; and 32 scans. (b) ^{13}C NMR spectroscopy: 39 mg; 3 s acquisition time; 4 s delay time; 5.5 μs pulse; spectral width 18 800 Hz, and more than 10 000 scans.

Size Exclusion Chromatography/Static Light Scattering (SEC/MALS): SEC/MALS measurements were performed at 30 °C on an Agilent 1200 system equipped with PLgel 5 μm Guard and PLgel 5 μm MIXED-C columns, a differential refractive index (RI) detector (Optilab Rex, Wyatt), and a SLS detector (Minidawn Treos, Wyatt). Data analysis was performed with ASTRA Software from Wyatt. Tetrahydrofuran (THF) was used as eluent at a flow rate of 1 mL min^{-1}. Values in THF were determined using Optilab Rex Detector. Samples were diluted in THF to a concentration of ≈5 mg mL^{-1} and filtered through a 0.45 mm nylon filter. The SEC setup consisted of a pump (LC-20A, Shimadzu), an autosampler (Waters 717), a differential refractometer (Waters 2410), and three columns in series

(Styragel HR2, HR4, and HR6 with pore sizes ranging from 102 to 106 Å). Chromatograms were obtained in THF at 35 °C using a flow rate of 1 mL min^{-1}. The equipment was calibrated using narrow polystyrene standards ranging from 595 to 3.95 × 10^6 g mol^{-1} (fifth-order universal calibration).

FTIR Spectroscopy: Infrared spectra were recorded at room temperature with a Thermo scientific model Nicolet 6700 FT-IR spectrometer, and KBr pellets were used for solid-state IR spectroscopy applying ten scans in transmission mode. For the calibration line and the graft copolymers pellets, 2.5 mg of the selected composition was diluted with 1 g of KBr. The mixture was mortered until the mixture was totally homogenized. Finally, the selected mixture was compressed forming a slightly black pellet that depends on the PEDOT composition.

Matrix-Assisted Laser Desorption Ionization-Time of Flight Mass Spectrometry: Analyses were performed on an Ultraflextreme III time-of-flight mass spectrometer equipped with a pulsed Nd:YAG laser (355 nm) and controlled by FlexControl 3.3 software (Bruker Daltonics, Bremen, Germany). The acquisitions (total of 2000–3000) were carried out in positive linear mode. A mixture of *trans*-2-[3-(4-*tert*-butylphenyl)-2-methyl-2-propenylidene] malonitrile (DCTB) and silver trifluoroacetate matrix was used to acquire the spectra. The polymer sample (PLA7K) was dissolved in THF at a concentration of 1 mg mL^{-1}. DCTB matrix was dissolved in THF at a concentration of 20 mg/ mL^{-1}, and 1 mg mL^{-1} silver trifluoroacetate (AgTFA) was added as cationic ionization agent. The samples were mixed with the matrix and salt at a 10:2:1 (matrix/sample/salt) ratio.

UV–vis–NIR Spectroscopy: UV–vis–NIR absorption spectra were recorded with a Perkin-Elmer UV–vis–NIR Lambda 950 spectrometer. To avoid saturation absorbance, 0.5 mg was diluted in 10 mL of chloroform ($CHCl_3$). The solution was sonicated for 15 min and then measured in a quartz cuvette.

Thermogravimetric Analyses: TGA was performed under nitrogen atmosphere (25 mL min^{-1} flow rate) using a TGA Discovery (TA Instruments). The procedure is composed of a first equilibration at 100 °C for 20 min and then heated at a rate of 10 °C min^{-1}, in the range from 100 to 800 °C. Air stability analysis was performed under air atmosphere (20 mL min^{-1}), isotherm of 110 °C during 120 °C.

Transmission Electron Microscopy: TEM images were collected using a JEOL JEM-2100F model EM-20014, which features a 200 kV field emission gun (FEG, Schottky) and an ultrahigh resolution (UHR) pole piece. To prepare the grid, 0.1 mg of the graft copolymer was solubilized in 1 mL of chloroform. The sample was sonicated for 15 min. Then 5 µL of the solution was deposited into a TEM grid and evaporated at room temperature.

Scanning Electron Microscope: Measurements were performed on JEOL JSM-6490LV at 5 kV, running in a point-by-point scanning mode. Previously, cylindrical coverslip with 11 mm diameter was introduced in isopropanol and sonicated for 15 min to remove impurities, solvent was evaporated at room temperature. A total of 25 mg of grafting PEDOT was solubilized in 1 mL of chloroform. Then, they were sonicated for 15 min and drop-casted in a cylindrical glass coverslip. The solvent was evaporated at room temperature. The samples were placed on an aluminum holder with double-side carbon tape and introduced in the SEM chamber. All the samples were evaluated at different magnifications.

Conductivity: The measurements of conductivity were performed on a four-point probe Ossila Sheet using more than three different zones of the film for more than three times. For this purpose, 100 µL of each dispersion were drop-casted in glass coverslips and dried at room temperature. The samples were prepared in the same way as SEM samples. First, the thickness of the drop-casting was measured using a digital caliper. Then the electrical conductivity was calculated taking into account the thickness of the sample.

Rheology measurement strain and frequency oscillatory experiments were carried out in an ARES rheometer (Rheometrics) at the melting temperature of the copolymers or macromonomers, i.e., 110 °C. Frequency sweeps studies of the different samples were carried out from 0.1 to 100 Hz at constant strain. Aluminum plates of 25 mm of diameter were used.

3D Printing: The printing process was carried out in a 3D-Bioplotter (Developer Series, EnvisionTEC, Gladbeck, Germany) and the printing geometries were originally designed in Autodesk Inventor 2019. Typically, the printing of the samples was performed at a temperature of 110 °C, with 0.001 mm of maximum resolution, and a maximum pressure of 4 × 10^5 Pa. In this study, needles with an inner diameter of 0.2 and 0.3 mm were used.

The polymer was printed at room temperature, so the temperature of the build platform was 20 °C. In the case of printing for the interlayer evaluation, PEDOT-*g*-PLA or PLA were deposited on Teflon sheet previously sprayed with commercially available hairspray. In contrast, PLA or PEDOT-*g*-PLA patterns for biological applications were printed onto glass coverslips previously coated with gelatin 5% v/v in water.

Isolation and in vitro culture of ventricular cardiomyocytes from neonatal mice (NMVM). Primary neonatal mouse ventricular cardiomyocytes (NMVMs) were isolated from 1 to 3-day-old C57BL/10SCSNJ mouse pups, following the previously described Pierce Primary Isolation Kit from Promega. Briefly, ventricles were separated from the atria using scissors, dissociated in HBFF buffer (calcium and bicarbonate-free Hanks buffer with HEPES), and digested with two specific enzymes provided by the Kit manufacturer for 30 min. Special media for cardiomyocytes enrichment was prepared with minimum essential media (DMEM), supplemented with 5% fetal bovine serum (FBS) and 0.5% Pen/Strep. Myocytes that were either in solution or lightly attached were then separated from the adherent stromal cells by gentle mechanical disaggregation and subsequently plated at a density of 2 × 10^5 cells mL^{-1} in primary petri dishes (Falcon) or in multichambered slides coated with 0.1% gelatin (Sigma). The resultant NMVMs were cultured (90k cells per sample) in 2D gelatin-coated plates (2D gelatin controls) or on the 3D-printed patterned substrates. After the first 24 h, culture medium was changed; afterward, cell culture medium was changed every 3 d. All the experiments were performed according to the Biodonostia Animal Care and Use Committee guidelines. Cell culture studies were repeated three times in quadruplicates for observation corroboration.

Immunofluorescence: NMVMs were fixed in phosphate buffered saline (PBS) containing 4% PFA for 15 min at room temperature. Cells were permeabilized at room temperature, with 1% Triton X-100 for 90 min, blocked with 2% BSA in PBS for 45 min and incubated overnight with α-sarcomeric actinin 1:400 (Sigma), to assess the contractile apparatus of NMVMs, and Vimentin 1:400 (Millipore), a cytoskeleton marker commonly used for fibroblast staining, prepared in 2% BSA. Goat anti-mouse antibody conjugated to Alexa Fluor 488 (Molecular Probes) and goat anti-chicken antibody conjugated to Alexa Fluor 647 (Invitrogen) were used as secondary antibody 1:400, respectively. Each sample was stained with Hoechst 1:2000 to counterstain the nuclei. Representative immunofluorescence images were acquired using an ECLIPSE Ti-S/L100 microscope (Nikon) equipped with a 20× S-Fluor objective and attached to a lambda-DG4 illumination system. For image processing, maximum intensity Z-projection images were generated using ZEN 2.3 software. Multiple images (at least 20) for each sample were taken to cover all the areas of the sample. For the quantification, fluorescence images were analyzed using an ImageJ program (National Institutes of Health, USA). In the analysis, the cells were counted by counting the number of nuclei and divided into two groups depending on the specific fluorescence given by each cell: sarcomeric actinin staining (green) specific for cardiomyocytes or vimentin for fibroblasts. Finally, the ratio is just the division between the number of CM/Fb.

Supporting Information

Supporting Information is available from the Wiley Online Library or from the author.

Acknowledgements

C.M.D.L.-A. wish to thank the grant 490946/279281 awarded by the Mexican Nacional Council of Science and Technology (CONACYT). This work was supported by funding from Health Institute Carlos III (ISCIII) funds and by Marie Sklowdowska-Curie Research and Innovation Staff Exchanges (RISE9 under Grant Agreement No. 823989.

Conflict of Interest

The authors declare no conflict of interest.

Data Availability Statement

The data that support the findings of this study are available from the corresponding author upon reasonable request.

Keywords

3D printing, cardiomyocytes, DIW, graft copolymers, PEDOT

Received: February 17, 2021
Revised: March 30, 2021
Published online: May 3, 2021

[1] A. M. Pekkanen, R. J. Mondschein, C. B. Williams, T. E. Long, *Biomacromolecules* **2017**, *18*, 2669.
[2] E. Sanchez-Rexach, T. G. Johnston, C. Jehanno, H. Sardon, A. Nelson, *Chem. Mater.* **2020**, *32*, 7105.
[3] B. Narupai, A. Nelson, *ACS Macro Lett.* **2020**, *9*, 627.
[4] M. P. A. Dominguez-Alfaro, N. Alegret, B. Arnaiz, J. M. González-Domínguez, A. Martin-Pacheco, U. Cossío, L. Porcarelli, S. Bosi, E. Vázquez, D. Mecerreyes, M. P. A. Dominguez-Alfaro, N. Alegret, B. Arna, A. Dominguez-Alfaro, N. Alegret, B. Arnaiz, J. M. González-Domínguez, A. Martin-Pacheco, U. Cossío, L. P. S. Bosi, E. Vázquez, D. Mecerreyes, M. Prato, **2020**.
[5] C. Diacci, J. W. Lee, P. Janson, G. Dufil, G. Méhes, M. Berggren, D. T. Simon, E. Stavrinidou, *Adv. Mater. Technol.* **2020**, *5*, 1900262.
[6] A. Williamson, J. Rivnay, L. Kergoat, A. Jonsson, S. Inal, I. Uguz, M. Ferro, A. Ivanov, T. A. Sjöström, D. T. Simon, M. Berggren, G. G. Malliaras, C. Bernard, *Adv. Mater.* **2015**, *27*, 3138.
[7] P. Leleux, C. Johnson, X. Strakosas, J. Rivnay, T. Hervé, R. M. Owens, G. G. Malliaras, *Adv. Healthcare Mater.* **2014**, *3*, 1377.
[8] D. Mantione, I. Del Agua, W. Schaafsma, J. Diez-Garcia, B. Castro, H. Sardon, D. Mecerreyes, *Macromol. Biosci.* **2016**, *16*, 1227.
[9] H. Yuk, B. Lu, S. Lin, K. Qu, J. Xu, J. Luo, X. Zhao, *Nat. Commun.* **2020**, *11*, 1604.
[10] D. N. Heo, S.e-J. Lee, R. Timsina, X. Qiu, N. J. Castro, L. G. Zhang, *Mater. Sci. Eng., C* **2019**, *99*, 582.
[11] E. Fantino, I. Roppolo, D. Zhang, J. Xiao, A. Chiappone, M. Castellino, Q. Guo, C. F. Pirri, J. Yang, *Macromol. Mater. Eng.* **2018**, *303*, 1700356.
[12] A. I. Hofmann, I. Östergren, Y. Kim, S. Fauth, M. Craighero, M.-H. Yoon, A. Lund, C. Müller, *ACS Appl. Mater. Interfaces* **2020**, *12*, 8713.
[13] E. Gkartzou, E. P. Koumoulos, C. A. Charitidis, *Manuf. Rev.* **2017**, *4*, 12.
[14] M. Mumtaz, E. Ibarboure, C. Labrugère, E. Cloutet, H. Cramail, *Macromolecules* **2008**, *41*, 8964.
[15] A. C. Da Silva, A. T. S. Semeano, A. H. B. Dourado, H. Ulrich, S. I. Cordoba De Torresi, *ACS Omega* **2018**, *3*, 5593.
[16] D. Mecerreyes, R. Stevens, C. Nguyen, J. A. Pomposo, M. Bengoetxea, H. Grande, *Synth. Met.* **2002**, *126*, 173.
[17] S. Marina, D. Mantione, K. Manojkumar, V. Kari, J. Gutierrez, A. Tercjak, A. Sanchez-Sanchez, D. Mecerreyes, *Polym. Chem.* **2018**, *9*, 3780.
[18] A. C. Da Silva, T. Augusto, L. H. Andrade, S. I. Córdoba De Torresi, *Mater. Sci. Eng., C* **2018**, *83*, 35.
[19] I. Zozoulenko, A. Singh, S. K. Singh, V. Gueskine, X. Crispin, M. Berggren, *ACS Appl. Polym. Mater.* **2019**, *1*, 83.
[20] A. C. Da Silva, M. J. Higgins, S. I. Córdoba De Torresi, *Mater. Sci. Eng., C* **2019**, *99*, 468.
[21] H. C. Chang, T. Sun, N. Sultana, M. M. Lim, T. H. Khan, A. F. Ismail, *Mater. Sci. Eng., C* **2016**, *61*, 396.
[22] W.-M. Chiu, H.-Y. Kuo, P.-A. N. Tsai, J.-H. Wu, *J. Polym. Environ.* **2013**, *21*, 350.
[23] D. Minudri, D. Mantione, D. Dominguez-Alfaro, A. Moya, S. Maza, E. Bellacanzone, C. Antognazza, M. R. Mecerreyes, *Adv. Electron. Mater.* **2020**, *6*, 2000510.
[24] J. Aho, J. P. Boetker, S. Baldursdottir, J. Rantanen, *Int. J. Pharm.* **2015**, *494*, 623.
[25] G. Vunjak-Novakovic, N. Tandon, A. Godier, R. Maidhof, A. Marsano, T. P. Martens, M. Radisic, *Tissue Eng., Part B* **2010**, *16*, 169.
[26] R. Dong, P. X. Ma, B. Guo, *Biomaterials* **2020**, *229*, 119584.